

SUPPORTING INFORMATION

A Distal Point Mutation in the Streptavidin-biotin Complex Preserves Structure but Diminishes Binding Affinity: Experimental Evidence for Electronic Polarization Effects?

Loren Baugh, Isolde Le Trong, David S. Cerutti, Susanne Gülich, Patrick S. Stayton, Ronald E. Stenkamp, Terry P. Lybrand

Departments of Bioengineering, Biological Structure and Biochemistry, University of Washington, Seattle, Washington 98195, and Center for Structural Biology and Department of Chemistry, Vanderbilt University, Nashville, Tennessee 37232

MATERIALS AND METHODS

Site-directed mutagenesis, protein expression, purification and characterization. The F130L mutation was created in the synthetic core streptavidin gene in pET21a (Novagen, San Diego, CA) using the QuikChange protocol (Stratagene, La Jolla, CA) as described previously (S1), and confirmed by sequencing. Protein was expressed using the T7 expression system in BL21(DE3) *E. coli* and purified as described previously (S2). The expected mass and purity of the mutants were confirmed using electrospray mass spectrometry. For protein concentration measurements, the molar extinction coefficient of F130L at 280 nm was reduced by a factor of 1.11 to account for the loss of the aromatic phenylalanine side chain. Melting temperature measurements for unbound WT and F130L using circular dichroism spectroscopy gave T_m values of 69.8 ± 1.1 and 64.3 ± 1.1 °C, respectively; F130L showed no measureable loss of secondary structure at the temperatures used in this study.

Kinetic measurements. The rate of biotin dissociation from streptavidin variants was measured using a cold-chase radiometric method described previously (S3). Briefly, 10 nM ^3H -biotin and 30 μM F130L or WT streptavidin in 50 mM sodium phosphate buffer, pH 7.0, 100 mM NaCl, were equilibrated at the experimental temperature for 2 h, at which point a large excess of unlabeled biotin (50 μM final concentration) was added and mixed rapidly. Two hundred microliter aliquots were removed periodically and immediately ultrafiltered using chilled, 30k Microcon filters (Millipore, Billerica, MA). The filtrate was counted to quantify the amount of ^3H -biotin released as a function of time.

Dissociation rate constants for protein-ligand complexes at each temperature were determined by fitting each data set by a one-term exponential decay. These k_{off} values were used to calculate initial estimates of ΔH^\ddagger and ΔS^\ddagger in a global fit of all data, with ΔH^\ddagger and ΔS^\ddagger as the only adjustable parameters, using the equation

$$I_t = I_0 \left\{ 1 - \exp \left[-\frac{k_B T}{h} \exp \left(\frac{T \Delta S^\ddagger - \Delta H^\ddagger}{RT} \right) \cdot t \right] \right\} \quad (1)$$

where I_t is the measured ^3H count at time t , I_0 is the initial ^3H count, k_B is Boltzmann's constant, h is Planck's constant, and R is the gas constant.

Equilibrium measurements: Competitive binding and calorimetry. Equilibrium binding enthalpies were measured at 12, 25 and 37 °C using a VP-ITC isothermal titration calorimeter (Microcal, Northampton, MA). Streptavidin at 30 μM in 50 mM sodium phosphate, pH 7.0, 100 mM NaCl, was titrated with 25 5- μL injections of 500 μM biotin. Heat flow was integrated and data was fit using Origin software.

Equilibrium binding affinity relative to WT streptavidin was determined using a radiometric competitive binding method described previously (S3). F130L at a range of concentrations (3-120 μM) competed with 50 nM WT streptavidin with a polyhistidine tag for 20 nM ^3H -biotin, in 50 mM sodium phosphate, pH 7.0, 100 mM NaCl, for 24 h at 37 °C. The partitioning of ^3H -biotin between proteins was measured by precipitating the his-tagged WT protein using nickel-nitrilotriacetic acid agarose resin (Qiagen, Valencia, CA) and counting ^3H -biotin remaining in solution. These counts, corrected for unbound ^3H -biotin, were fit as the root of the competitive binding equation

$$\frac{K_C}{K_P} \cdot [C \cdot L] + \left(L_T + C_T + \frac{K_C}{K_P} (P_T - L_T) \right) \cdot [C \cdot L] - L_T C_T = 0 \quad (2)$$

where K_C and K_P are the equilibrium dissociation constants for the competitor and WT, respectively, and $[C \cdot L]$, L_T , C_T and P_T are the concentrations of competitor-bound ligand, total ligand, total competitor, and total WT protein, respectively.

Crystallization. The F130L mutant of “core” streptavidin (S4) was co-crystallized with biotin using hanging drop vapor diffusion techniques. Crystals were obtained by mixing protein at 25 mg/mL with a two-fold molar excess of biotin in water. The reservoir solution was 0.1 M HEPES, pH 7.5 with 16% PEG 8000. Drops of protein and ligand solution were mixed with an equal volume of reservoir solution before equilibration. Crystals were transferred to a crystallization solution containing 30% glycerol as a cryoprotectant.

Diffraction data collection. Diffraction data were collected at the Swiss Light Source ($\lambda = 1.0 \text{ \AA}$) at 100K using a Pilatus detector and processed with XDS software (S5). The space group for the crystals is $P2_1$, with a streptavidin tetramer in the asymmetric unit. Data set statistics are shown in Table 1a.

Structure solution and refinement. The crystal structure of F130L was obtained from the isomorphous structure of the double mutant S45A/D128A of core-streptavidin (PDB ident 1MEP) (S6). The structural model was refined using REFMAC-5 (S7) in the CCP4 suite (S8). R_{free} (S9) was calculated using 5% of the data in the test set. All atoms were refined with anisotropic temperature factors. Riding hydrogen atoms were added to the model, and Babinet scaling was used to account for bulk solvent effects.

Sigma A weighted $|F_{\text{ol}}| - |F_{\text{cl}}|$ and $2|F_{\text{ol}}| - |F_{\text{cl}}|$ electron density maps (S10) were viewed with XtalView (S11) for graphical evaluation of the model and electron density maps. XtalView, MOLSCRIPT (S12), and Raster3d (S13) were used to produce the structural figures for this paper.

The final structural model consists of four streptavidin subunits (chain A: residues 16-134, B:16-135, C:16-135, D:16-135), four biotin molecules, 510 fully-occupied oxygen atoms for water molecules, 20 partially-occupied waters, and 11 glycerol molecules. MolProbity (S14) was used for model validation. Table S1b contains refinement statistics for the structure. Coordinates and structure factors have been deposited for the F130L mutant in the Protein Data Bank with identifier 3MG5.

Molecular dynamics simulations. Starting coordinates for the simulations were taken from the current x-ray structure. The eight histidine residues in the tetramer were singly protonated to model the ionization state expected for a neutral solution. Hydrogen atoms were added to all protein heavy atoms using the Leap module in AMBER 9 (S15). The full complex was solvated in a truncated octahedral box containing 19,584 water molecules, and eight sodium counterions were added to maintain charge neutrality for the system.

The simulation methods and protocol are comparable to that reported previously for solution phase simulations of WT streptavidin (S16). Briefly, all calculations were performed using the AMBER ff99 force field (S17, S18) with modifications by Simmerling and co-workers (S19), the SPC/E water model (S20) and a sodium cation model from Åqvist (S21). Biotin parameters were taken from previous work by

Israilev and co-workers (S22). Force calculations were performed with periodic boundary conditions, a 9.0°Å cutoff on real space interactions, a homogeneity assumption to approximate the contributions of long-range Lennard-Jones forces to the virial tensor, and smooth particle-mesh Ewald electrostatics (S23). The SHAKE algorithm (S24) was used to constrain the lengths of all bonds to hydrogen atoms and the SETTLE algorithm (S25) was used to constrain the internal geometry of all rigid SPC/E water molecules. A Langevin thermostat (S26) with collision frequency 3 ps⁻¹ was used to maintain the system temperature. All energy minimizations and dynamics were performed with the PMEMD module of AMBER 9 (S15). To avoid artifacts arising from reuse of particular sequences of random numbers (S27), the random number generator seed was incremented with every restart of the dynamics.

To prepare the system for equilibrium MD simulations, hydrogen atoms, water molecules and sodium atoms were first relaxed by 2000 steps of steepest-descent energy minimization while crystallographically resolved protein atoms were held in place by 1000 kcal/mol-Å² position restraints. The protein heavy atoms were then energy minimized while solvent particles were tightly restrained to their new positions, and finally all components of the system were energy-minimized with no restraints. Restrained dynamics of the system were conducted for a total of 450 ps, beginning with a 0.5 fs time step in the constant volume, constant temperature ensemble and 16.0 kcal/mol-Å² restraints on all crystallographically observed protein atoms. The restraints were gradually reduced to 1.0 kcal/mol-Å² over the first 150 ps before switching to the constant pressure ensemble, increasing the time step to 1.5 fs, and reducing the restraints to 0.0625 kcal/mol-Å² over the next 300 ps. Production dynamics were propagated in the constant pressure ensemble with a 1.5 fs time step for 500 ns with no position restraints.

Quantum mechanical calculations. All quantum mechanical calculations were performed with the Gaussian 09 package (S28) at the Hartree-Fock level of theory with a 6-31g(d,p) basis set. The active site model was extracted from the current x-ray crystal structure, and hydrogen atoms were added and refined using the procedure described above for the molecular dynamics preparation. The C α positions for residues N23, S27, Y43, S45, and D128 were restrained at their relative crystallographic positions to maintain the general binding site geometry, and all other atoms were allowed to move freely during the geometry optimization calculations. All optimized structures were verified as local minima with frequency calculations.

RESULTS

Table S1a. Crystallographic data collection statistics

Unit cell dimensions (a,b,c, β)	50.9, 97.5, 52.7, 112.3
Space group	P2 ₁
Resolution	50.0-1.17 Å (1.35-1.17)
Unique reflections	121722
Completeness (last shell)	76.0% (14.5%)
Redundancy (last shell)	4.6 (2.1)
I/sigma (last shell)	14.1 (0.7)
R _{merge} (last shell)	0.057 (0.836)

Table S1b. Refinement statistics

Resolution	48.7-1.3 Å (1.33-1.30 Å)
R factor (overall)	0.134
R factor (working set)	0.132 (0.217)
R _{free} (test set = 5% of overall)	0.178 (0.255)

# unique reflections	104826
Average B value (protein)	17.7 Å ²
Average B values (biotins)	13.2 Å ²
Average B values (glycerols)	29.5 Å ²
Average B values (water molecules)	30.1 Å ²
Ramachandran quality	
% of residues in favored regions	97.5%
in allowed regions	100%
rms deviation - bond lengths	0.012 Å
- bond angles	1.57 °

Superimposing the A subunits of the two structures (liganded F130L and WT (pdb 1MK5)) using 98 C α atoms of the subunit core gives an RMSD value of 0.377 Å. Similar values (0.427 Å, 0.439 Å, and 0.437 Å) were obtained for superimposing the A subunit of 1MK5 onto subunits B, C and D of F130L, and for superimposing the B subunit of 1MK5 onto the four subunits of F130L (0.395 Å, 0.292 Å, 0.377 Å, and 0.371 Å).

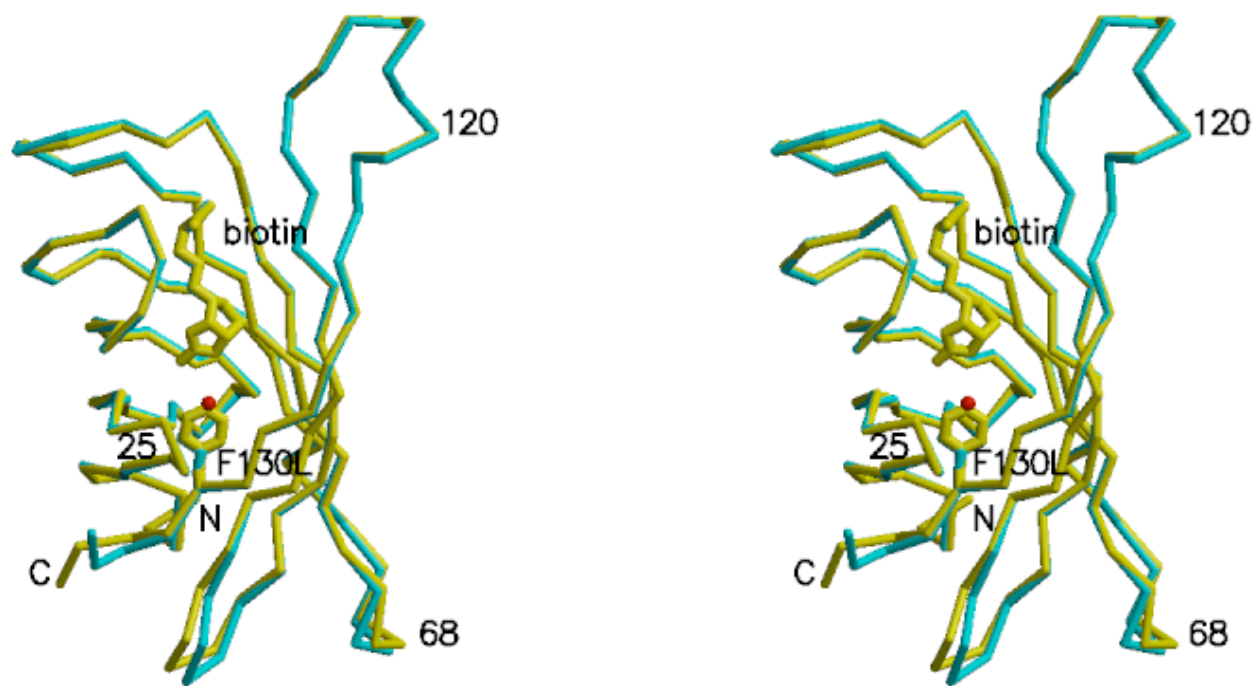


FIGURE S1: Stereoview of superposition of bound WT (yellow) and F130L (blue) overall structures.

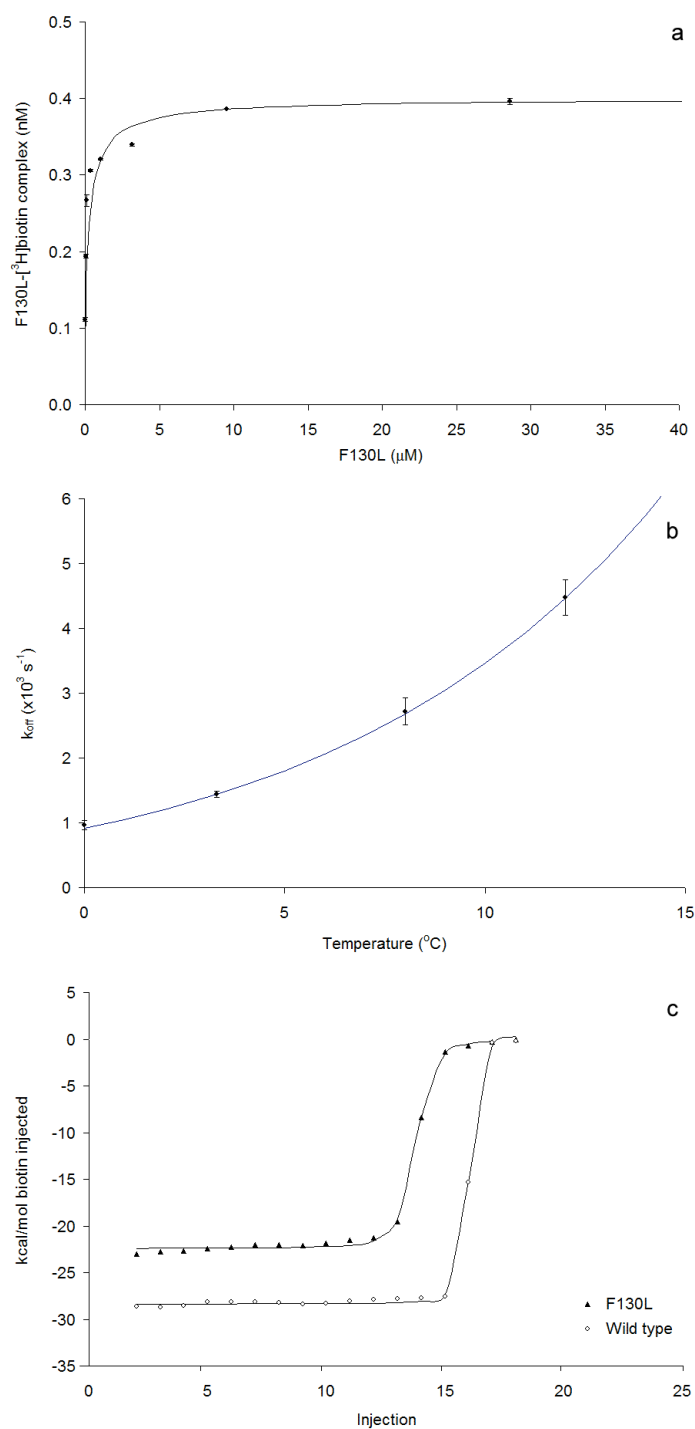


FIGURE S2: Effect of F130L mutation on biotin binding affinity and thermodynamics. (a) Competitive binding of F130L with WT streptavidin (50 nM) for ³H-biotin (20 nM) at 37 °C. F130L displays a 975-fold reduction in binding affinity relative to WT ($\Delta\Delta G^\circ = 4.2$ kcal/mol). (b) The temperature dependence of biotin dissociation from F130L was used to determine thermodynamic activation parameters, ΔH^\ddagger and ΔS^\ddagger , by fitting data to an Eyring model. Biotin dissociation is 7600-fold faster for F130L than for WT streptavidin at 12 °C, and was too fast to measure above 12 °C. (c) Calorimetric titration curves for F130L and WT streptavidin titrated with biotin at 37 °C, show a reduced enthalpy of binding for F130L ($\Delta\Delta H^\circ$) of 5.5 kcal/mol. $\Delta\Delta G^\circ = \Delta\Delta H^\circ - T\Delta\Delta S^\circ$ yields a more favorable entropy of binding for F130L ($T\Delta\Delta S^\circ$) of 1.3 kcal/mol.

REFERENCES

- S1. Hyre, D., Le Trong, I., Freitag, S., Stenkamp, R. E., and Stayton, P. S. (2000) *Protein Sci.* 9, 878-885.
- S2. Chilkoti, A., Tan, P., and Stayton, P. S. (1995) *Proc. Natl. Acad. Sci. U S A* 92, 1754-1758.
- S3. Klumb, L., Chu, V., and Stayton, P. S. (1998) *Biochemistry* 37, 7657-7663.
- S4. Sano, T., Pandori, M., Chen, X., Smith, C., and Cantor, C. (1995) *J. Biol. Chem.* 270, 28204-28209.
- S5. Kabsch, W. (1993) *J. Appl. Cryst.* 26, 795-800.
- S6. Hyre, D., Le Trong, I., Merritt, E. A., Eccleston, J. F., Green, N. M., Stenkamp, R. E., and Stayton, P. S. (2006) *Protein Sci.* 15, 459-467.
- S7. Murshudov, G. N., Vagin, A. A., and Dodson, E. J. (1997) *Acta Cryst. D*53, 240-255.
- S8. Collaborative Computational Project, N. (1994) *Acta Cryst. D*50, 760-763.
- S9. Brünger, A. T. (1993) *Acta Cryst. D*49, 24-36.
- S10. Read, R. J. (1986) *Acta Cryst. A*42, 140-149.
- S11. McRee, D. E. (1999) *J. Struct. Biol.* 125, 156-165.
- S12. Kraulis, P. J. (1991) *J. Appl. Crystallogr.* 24, 946-950.
- S13. Merritt, E. A., and Bacon, D. J. (1997) *Meth. Enzym.* 277, 505-524.
- S14. Davis, I. W., Leaver-Fay, A., Chen, V. B., Block, J. N., Kapral, G. J., Wang, X., Murray, L. W., Arendall, W. B. I., Sinoeyink, J., Richardson, J. S., *et al.* (2007) *Nucl. Acids Res.* 35, W375-W383.
- S15. Case, D. A., Cheatham, T. E., Darden, T. A., Gohlke, H., Luor, R., Merz, M., Onufriev, A., Simmerling, C., Wang, B., Woods, R. (2005) *J. Comput. Chem.* 26, 1668-1688.
- S16. Cerutti, D. S., Le Trong, I., Stenkamp, R. E., and Lybrand, T. P. (2009) *J. Phys. Chem. B* 113, 6971-6985.
- S17. Cornell, W. D., Cieplak, P., Bayly, C. I., Gould, I. R., Merz, K. M., Jr., Ferguson, D. M., Spellmeyer, D. C., Fox, T., Caldwell, J. W., Kollman, P. A. (1995) *J. Am. Chem. Soc.* 117, 5179-5197.
- S18. Wang, J., Cieplak, P., Kollman, P. A. (2000) *J. Comput. Chem* 21, 1049-1074.
- S19. Hornak, V., Abel, R., Okur, A., Strockbine, B., Roitberg, A., Simmerling, C. (2006) *Proteins* 65, 712-725.
- S20. Berendsen, H. J. C., Grigera, J. R., Straatsma, T. P. (1987) *J. Phys. Chem.* 91, 6269-6271.
- S21. Åqvist, J. (1990) *J. Chem. Phys.* 94, 8021-8024.
- S22. Israilev, S., Stepaniants, S., Balsera, M., Oono, Y., Schulten, K. (1997) *Biophys. J.* 72, 1568-1581.
- S23. Essmann, U., Perera, L., Berkowitz, M. L., Darden, T., Lee, H., Pedersen, L. H. (1995) *J. Chem. Phys.* 103, 8577-8593.
- S24. Ryckaert, J. P., Ciccotti, G., Berendsen, H. J. C., Hirasawa, K. (1997) *J. Comput. Phys.* 23, 327-341.
- S25. Miyamoto, S., Kollman, P. A. (1992) *J. Comput. Chem.* 13, 952-962.
- S26. Izaguirre, J. A., Catarello, D. P., Wozniak, J. M., Skeel, R. D. (2001) *J. Chem. Phys.* 114, 2090-2098.
- S27. Cerutti, D. S., Duke, R. E., Freddolino, P. L., Fan, H., Lybrand, T. P. (2008) *J. Chem. Theory Comput.* 2008, 4, 1669-1680.
- S28. Gaussian 09, Revision A.02, Frisch, M. J.; Trucks, G. W.; Schlegel, H. B.; Scuseria, G. E.; Robb, M. A.; Cheeseman, J. R.; Scalmani, G.; Barone, V.; Mennucci, B.; Petersson, G. A.; Nakatsuji, H.; Caricato, M.; Li, X.; Hratchian, H. P.; Izmaylov, A. F.; Bloino, J.; Zheng, G.; Sonnenberg, J. L.; Hada, M.; Ehara, M.; Toyota, K.; Fukuda, R.; Hasegawa, J.; Ishida, M.; Nakajima, T.; Honda, Y.; Kitao, O.; Nakai, H.; Vreven, T.; Montgomery, Jr., J. A.; Peralta, J. E.; Ogliaro, F.; Bearpark, M.; Heyd, J. J.; Brothers, E.; Kudin, K. N.; Staroverov, V. N.; Kobayashi, R.; Normand, J.; Raghavachari, K.; Rendell, A.; Burant, J. C.; Iyengar, S. S.; Tomasi, J.; Cossi, M.; Rega, N.; Millam, N. J.; Klene, M.; Knox, J. E.; Cross, J. B.; Bakken, V.; Adamo, C.; Jaramillo, J.; Gomperts,

R.; Stratmann, R. E.; Yazyev, O.; Austin, A. J.; Cammi, R.; Pomelli, C.; Ochterski, J. W.; Martin, R. L.; Morokuma, K.; Zakrzewski, V. G.; Voth, G. A.; Salvador, P.; Dannenberg, J. J.; Dapprich, S.; Daniels, A. D.; Farkas, Ö.; Foresman, J. B.; Ortiz, J. V.; Cioslowski, J.; Fox, D. J. Gaussian, Inc., Wallingford CT, 2009.